



Received: 16-04-2023

Revised: 12-05-2023

Accepted: 07-06-2023

## Optimal Attention based Deep Learning with Segmentation Approach for Automated Leukemia Detection and Classification

**I.Vinurajan<sup>1</sup>, Dr. K. P. SanalKumar<sup>2</sup>, Dr. S. Anu HNair<sup>3</sup>**

<sup>1</sup>Research Scholar, Department of Computer and Information Sciences, Annamalai University, Chidambaram, India.

<sup>2</sup>Assistant Professor, PG Department of Computer Science, R.V Government Arts College, Chengalpattu, India.

<sup>3</sup>Assistant Professor, Department of CSE, Annamalai University, Chidambaram, India  
[Deputed to WPT, Chennai].

E-Mail: <sup>1</sup>nivinrajan01@gmail.com, <sup>2</sup>sanalprabha@yahoo.co.in, <sup>3</sup>anu\_jul@yahoo.co.in

### Abstract

Leukemia is a deadly disease that compromises the exists of numerous people worldwide. Leukemia does not form strong cancers, yet constitutes a considerable amount of anomalous white platelets that cluster out the typical platelets. Hematologists analyze blood smears from people to detect this anomaly appropriately. The method utilized for diagnoses is impacted by various factors such as the level of weariness and the hematologist's experience, which leads to inaccuracies and nonstandard results. Automatic analysis of acute lymphoblastic leukemia (ALL) is a vital and difficult task. Presently, machine learning (ML) and deep learning (DL)-based identification have become a commendable means in medical image analysis. DL algorithm is mainly utilized in leukemia treatment, for identifying if leukemia exists in a patient. In this work, we propose an Optimal Attention-based DL with Segmentation for Automated Leukemia Detection and Classification (OADLS-ALDC) technique. The OADLS-ALDC technique primarily undergoes image pre-processing in two phases: Wiener Filter (WF) and Dynamic Histogram Equalization (DHE). At the same time, the Watershed Segmentation approach is applied to segment the pre-processed images. Next, the OADLS-ALDC technique uses EfficientNetV2M for the identification of useful feature vectors. Moreover, the recognition and identification of leukemia takes place by the use of the Attention Convolutional Recurrent Neural Network (ACRNN) model. Furthermore, the hyperparameter selection of the ACRNN model is performed using a root mean square propagation (RMSProp) Optimizer. To highlight the improved detection outcomes of the OADLS-ALDC system, a sequence of experiments was involved. The experimental values identified that the OADLS-ALDC approach gets better performance than other techniques.



Received: 16-04-2023

Revised: 12-05-2023

Accepted: 07-06-2023

**Keywords:** Leukemia Detection; Deep Learning; EfficientNetV2M; RMSProp; White Blood Cells

## 1. Introduction

Leukemia is one of the types of cancer with high rates of mortality. It is attended by the malicious cloning of irregular white blood cells (WBC) and therefore is represented as a malignant cancer [1]. Generally, WBC, red blood cells (RBC), and platelets are the human body has 3 different sorts of cells. The oxygen supply from the heart to each tissue is often the responsibility of RBC [2]. Similarly, the WBC acts as a protection wall from various diseases and plays an important part in the immune system. Consequently, the accurate classification of these WBCs is crucial to determine the disease nature [3]. They are divided based on the cytoplasm composition. Lymphocytes are the classes of WBC and their diseases cause Acute Lymphoblastic Leukemia (ALL). In general, chronic and acute leukemia are dual subclasses of leukemia [4]. The preliminary stage of chronic leukemia is more than ALL, while the recovery amount of ALL is hardly 3 months without any treatment. ALL is the ubiquitous category of ALL accounting for around 25% of childhood tumors [5]. It appears in the lymphatic system that produces the blood cells. In the early stages, it originates in the bone marrow and consequently spreads all over the body [6]. The WBC growth relies mainly on the requirement of the body in the healthy individual, but when it comes to leukemia, they are abnormally formed while losing their effectiveness.

A microscopic blood test is considered the primary method for leukemia diagnosis [7]. The most widely used technique for discovering leukemia is the analysis of blood smears. Interventional radiology is an alternate approach for leukemia diagnoses. However radiological methods like catheter drainage, percutaneous aspiration, and biopsy, can be influenced by the resolution of the radio images and inheriting limitations of imaging modality sensitivity [8]. Microscopic blood tests and bone marrow are the widely adopted strategies for the detection of leukemia subtypes due to the cost requirements and time of these techniques. Machine learning (ML) techniques assist in detecting the blood cells with leukemia from the healthy cells when a large set of training is available [9]. There is a need for hematologists to detect leukemia's existence together with its certain form to determine the correct leukemia treatment and to prevent medical risks. A time-consuming and crucial step is the detection of leukemia through the examination of optical blood smears monitored by hematologists. To resolve these problems, several CAD methods for quantitative analysis of the peripheral blood samples have been projected with the help of deep learning and machine learning algorithms [10]. But this approach has certain disadvantages and it is necessary to improve efficiency, accuracy, and learning process.



Received: 16-04-2023

Revised: 12-05-2023

Accepted: 07-06-2023

This study proposes an Optimal Attention-based Deep Learning with Segmentation for Automated Leukemia Detection and Classification (OADLS-ALDC) technique. The OADLS-ALDC technique primarily undergoes image pre-processing in two phases: Wiener Filter (WF) and Dynamic Histogram Equalization (DHE). Next, the OADLS-ALDC technique uses EfficientNetV2M for the identification of useful feature vectors. Moreover, the recognition and identification of leukemia takes place by the use of the Attention Convolutional Recurrent Neural Network (ACRNN) model. Furthermore, the hyperparameter selection of the ACRNN model is performed using a root mean square propagation (RMSProp) Optimizer. To highlight the enhanced detection results of the OADLS-ALDC system, a sequence of experiments was involved. The experimental values identified that the OADLS-ALDC method obtains better performance than other approaches.

## 2. Literature Review

Ghongade et al. [11] recommend a DL and TL-based model for forecasting ALL blood cells. The projected model utilizes a pre-trained CNN technique to remove relevant features from the microscopic imageries of blood cells throughout the FE stage. To precisely classify it, an identification method is constructed utilizing a TL model using the composed features. MoradiAmin et al. [12] projected an effective and precise automatic model to differentiate ALL cells from the parallel lymphocyte sub-types without the necessity for straight FE. Initially, the contrast of microscopic imageries was improved by utilizing histogram equalization that enhances the reflectivity of significant features. Then, a fuzzy C-means clustering system has been utilized to fragment cell nuclei, as they play a vital part in ALL analyses. Lastly, a new CNN with 3 convolutional layers is used to categorize the segmented nuclei. In [13], a hybrid technique is projected utilizing a GA and a ResNet-50V2, residual CNN, to forecast ALL utilizing microscopy imageries accessible in the dataset of ALL-IDB. This work utilizes GA to discover the finest hyperparameter that main to the maximum rate of accuracy in the methods.

In [14], methods with higher efficiency and accuracy were proposed. In all projected methods, blood micrographs were enhanced and served as the active contour technique to remove WBC-only areas for additional diagnosis by 3 CNN methods. Similarly, CNN was served to the PCA technique to pick extremely representative features and referred to XGBoost and RF classifiers for identification. Awais et al. [15] projected an enhanced pipeline for dual recognition and sub-type identification of ALL from blood smear imageries. Initially, a customized, 88-layer deep CNN was developed and trained to utilize TL beside GoogleNet CNN to generate an ensemble of features. Also, this paper replicas the FS issue as a combinatorial optimizer issue and suggests a memetic form of dual WOA.



Received: 16-04-2023

Revised: 12-05-2023

Accepted: 07-06-2023

Abunadi and Senan [16] intended to progress diagnostic methods. It involves 3 projected methods are depend upon hybrid features removed utilizing GLCM, FCH, and LBP techniques. The 2nd projected model contains the CNN methods based on the TL method. The 3rd developed method contains hybrid CNN–SVM technologies, containing dual blocks: CNN methods for removing feature maps and the SVM system for categorizing feature maps. Khan et al. [17] proposed a higher-performance CNN joined with a two-attention system that proficiently identifies and categorizes WBCs in microscopic imageries. In the developed model, a DCGAN approach is employed to overwhelm the restrictions executed by restricted training data and use a binary attention mechanism.

### 3. The Proposed Method

In this work, we projected an OADLS-ALDC system. The main purpose of the OADLS-ALDC technique approach contains different kinds of processes involved as image processing, segmentation, feature extraction, ACRNN-based detection, and parameter selection. Fig. 1 illustrates the entire flow of the OADLS-ALDC technique.

#### 3.1. Image Pre-processing

Primarily, the OADLS-ALDC method undergoes image pre-processing in dual phases: WF and DHE. The WF is a linear filter that minimizes the MSE between the filtered and the original signals [18]. It enhances images corrupted by the noise. The WF is used to preservation of important image details and balance noise reduction by adjusting the filter parameters.

$$\hat{S}(u, v) = G(u, v)X(u, v) \quad (1)$$

$$G(u, v) = \frac{H * (u, v)P_S(u, v)}{|H(u, v)|^2 + \frac{P_S(u, v)}{P_n(u, v)}} \quad (2)$$

$$G(u, v) = \frac{H * (u, v)}{|H(u, v)|^2 + \frac{P_n(u, v)}{P_S(u, v)}} \quad (3)$$

Here,  $P_S(u, v)$  and  $P_n(u, v)$  are the power spectrum of the signal and noise procedures.



Received: 16-04-2023

Revised: 12-05-2023

Accepted: 07-06-2023

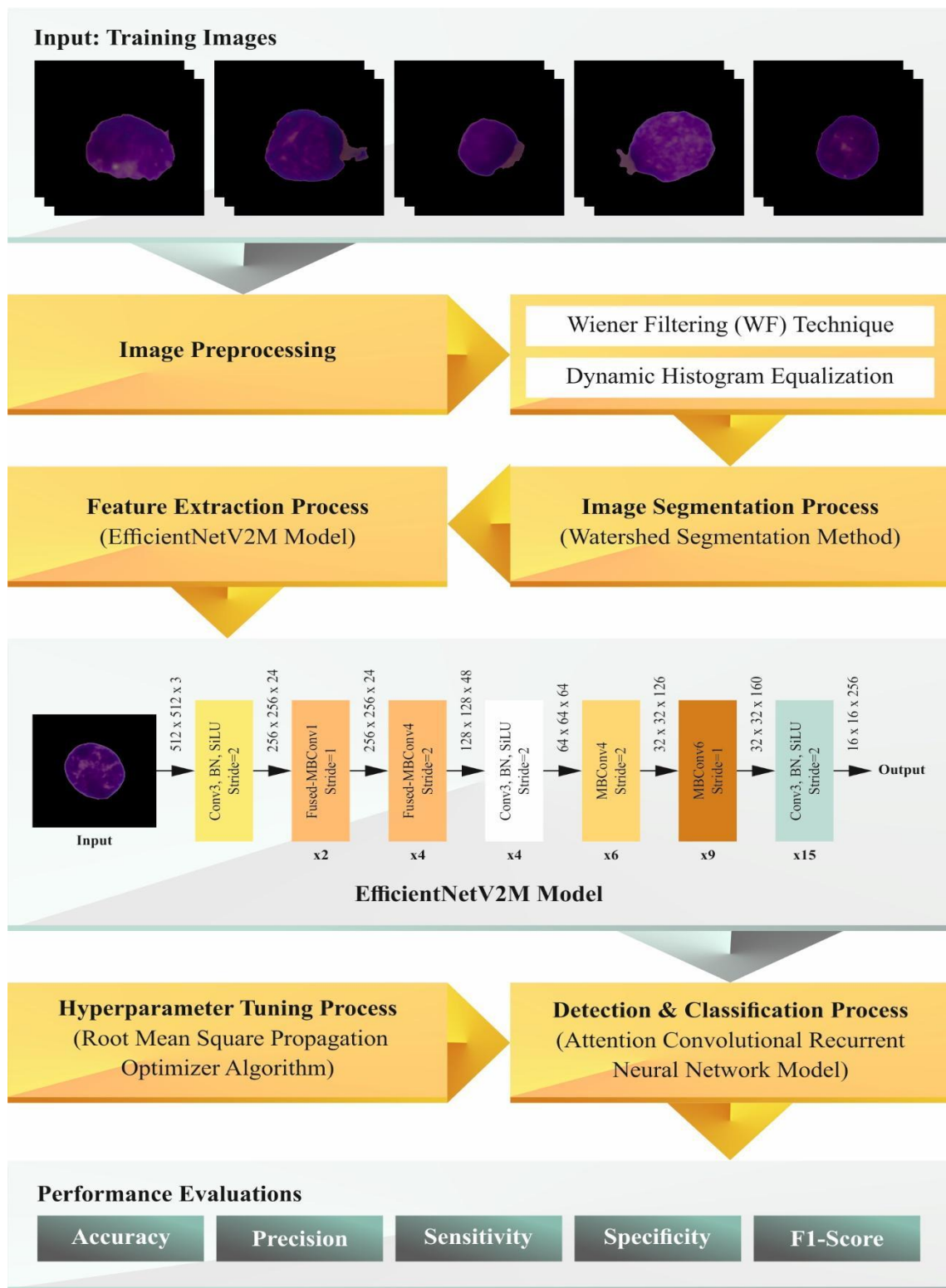


**Fig. 1.** Overall flow of OADLS-ALDC technique



Received: 16-04-2023

Revised: 12-05-2023

Accepted: 07-06-2023

DHE is a powerful method in medical imaging for improving the interpretability and quality of images [19]. Unlike conventional histogram equalization models, DHE functions dynamically, altering the intensity distribution of pixels depending on their local context rather than the complete image. This adaptability permits DHE to efficiently address variants in contrast and illumination within medical imageries, thus improving the accuracy of diagnostics. By analyzing and adjusting the histogram of smaller areas within the image, DHE maintains significant details and enhances complete contrast. In medical applications like pathology and radiology, where subtle features can considerably impact analysis and treatment planning, DHE is helpful in the recognition of complex anatomical structures, abnormalities, and lesions that may or else stay covered.

### 3.2. Watershed Segmentation

At the same time, the Watershed Segmentation approach is employed in order to segment the pre-processed images. The watershed segmentation is developed based on internal and external marking constraints and gradient images [20]. Mostly, the excessive noise and regional extrema were removed by the gradient image, therefore, the over-segmentation phenomenon was considerably enhanced. In addition, the contour positioning skill decreases the location deviance of the local contour line. Nevertheless, few target point has no connection with the object of interest. So, the object of interest is divided into meaningless minimum target points. If the object of interest is attained before the transformation of watershed segmentation, these objects suppress the meaningless small area, therefore over-segmentation is eliminated. The gradient imagery implements the minimum marking according to  $OC_b^{(rec)}$  and makes the marker a minimum regional for conducting the segmentation of the watershed.

In summary, the segmentation procedure of the decomposed region is given as: (1) calculate the morphological gradient of the filtered images; (2) perform morphological filter for target images; (3) perform the marker-based watershed transformation on the gradient imagery and (4) reconstruct the gradient image.

### 3.3. Feature Extraction Models

Next, the OADLS-ALDC technique uses EfficientNetV2M for the identification of useful feature vectors. The baseline EfficientNet structure depends upon a novel scaling model for enhancing volume by measuring the sizes of width, depth, and resolution utilizing a simple compound coefficient. Neural Architecture Search (NAS) is employed to project a novel baseline technique utilizing BConv blocks and measure it utilizing the compound coefficient to generate EfficientNet [21]. This novel family of methods attains advanced performance on a dataset of ImageNet while consuming a far lesser method and faster converging speed. This family is then enhanced even additional by using Fused-MBConv. The novel and enhanced



Received: 16-04-2023

Revised: 12-05-2023

Accepted: 07-06-2023

methods are then named EfficientNet V2, which with an exact training technique, can attain  $5\times - 11\times$  faster-converge speed when equated to other advanced techniques with up to  $6\times$  lesser in size. EfficientNetV2 executed in this work was B0 and M version. EfficientNet V2B0 has an improved trade-off on precision and FLOPs, whereas EfficientNet V2M decreases parameters and FLOP but runs quicker in training and inference when equated to version V1-B7.

EfficientNet V2M contains 740 layers which are utilized to increase the accuracy in identifying dissimilar kinds of tomato leaf illnesses. In the early phase, a novel layer is inserted containing a fully connected (FL) layer by the amount of labels as per the kind of illness to be identified. Then, the top layer is frozen so it cannot be altered or retrained.

### 3.4. Leukemia Detection Using ACRNN Model

At this stage, the recognition and identification of leukemia takes place through the use of the ACRNN model. Firstly, CNN learns feature representation [22]. Second, the features are inputted to the Bi-GRU layer which learns the temporal relationship. Lastly, this feature is fed into an FC layer with the softmax to yield the spreading of various classes. Here, the convolution RNN has 8 convolution layers ( $l_1 - l_8$ ) and 2 Bi-GRU layers ( $l_9 - l_{10}$ ) which are given below:

- $l_1-l_2$ : The 1<sup>st</sup> 2 stacked convolution layers exploit 32 filters with the receptive area of (3,5) and stride of (1,1). It follows the max-pooling with  $a(4,3)$  stride for reducing the sizes of the feature map. ReLu is applied.
- $l_3-l_4$ : Then dual convolution layers exploit 64 cells with the receptive area of (3,1) and stride of (1,1), and learn local features alongside the frequency size. It follows the max-pooling with  $a(4,1)$  stride. ReLu is applied.
- $l_5-l_6$ : The subsequent set of convolution layers exploits 128 cells with the receptive area of (1,5) and stride of (1,1) and learns local features alongside the time dimension. It follows a max-pooling with a stride of  $a(1,3)$ . ReLu is employed.
- $l_7-l_8$ : The following dual convolution layers utilize 256 cells with the receptive area of (3,3) and stride of (1,1) for learning joint time-frequency. It follows a max-pooling of  $a(2,2)$  stride. ReLu was applied.
- $l_9-l_{10}$ : Dual Bi-GRU layers with 256 filters were utilized for time-based correlation, and the tanh was applied.

BN has employed convolution layers of output to accelerate training. L2-normalization was used for the weights of all the layers with a co-efficient 0:0001.



Received: 16-04-2023

Revised: 12-05-2023

Accepted: 07-06-2023

The attention model was intended to perfect the relative proportion of every pixel of the  $T$  regional feature map [23]. Mainly, in the reasoning process, it identifies noticeable regions from the image region. The attention module is proposed by the  $\lambda_t$  term (regional attention map) that controls the pixel contribution of at  $t^{th}$  state and is trained by the NN. A large  $\lambda_t$  values indicate high importance. The attention function  $g: \delta_t, h_{t-1} \rightarrow \varepsilon_t$  is described by:

$$\zeta_t = \{\tanh(\delta_t W_\delta + h_{t-1} W_h)\} W_a \quad (4)$$

$$\lambda_t = \text{softmax}(\zeta_t) \quad (5)$$

$$\varepsilon_t = g(\delta_t, h_{t-1}) = \sum_{ij} \lambda_{t,ij} \cdot \delta_{t,ij} \quad (6)$$

Here  $W_\delta \in R^{C \times C}$ ,  $W_h \in R^{E \times C}$ ,  $W_a \in R^{C \times 1}$  denotes the matrices of embedding,  $E$  refers to the dimensional of the GRU unit, and  $\delta_{t,ij}$  shows  $t^{th}$  regional feature maps at  $(i, j) \in H' \times W'$ .  $\varepsilon_t$  indicates the output depiction for the  $t^{th}$  regional feature map. Fig. 2 represents the framework of ACRNN.

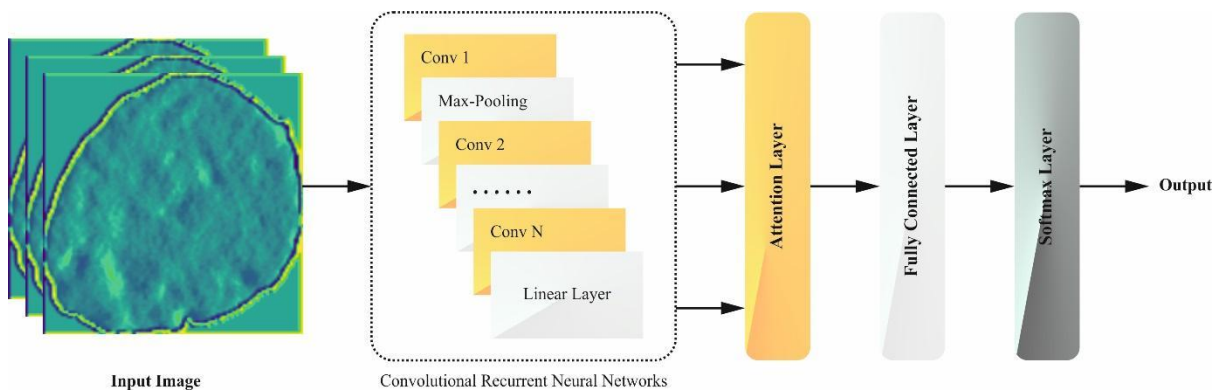


**Fig. 2.** Architecture of ACRNN

### 3.5. Parameter Selection Process

At last, the hyperparameter selection of the ACRNN model is performed using RMSProp Optimizer. The SDG algorithm RMSprop adjusts the learning rate for all the weights according to the average magnitude of the existing gradient for that weight [24]. It exploits an exponentially decayed average for calculating these magnitudes, providing more weight to existing gradients than the old one. This allows fast convergence towards the optimum solution and prevents the learning rate from oscillating. The square gradient is accumulated to apply RMSprop after calculating the gradient.



Received: 16-04-2023

Revised: 12-05-2023

Accepted: 07-06-2023

$$r \leftarrow \rho r + (1 - \rho) g \mathcal{S}g \quad (7)$$

Where the rate of deterioration is  $r$ . The parameter update is given by:

$$\Delta \theta = - \sqrt{\frac{\epsilon}{\delta + r}} \mathcal{S}g \quad (8)$$

$$\theta \leftarrow \theta + \Delta \theta \quad (9)$$

The fitness function (FF) is the major feature of deploying the solution of RMSProp Optimizer. The hyperparameter assortment procedure covers the performance-encoded system to evaluate the efficiency of the candidate's performance. In this work, the RMSProp Optimizer reflects accuracy as the main standard to design the FF that is expressed below.

$$Fitness = \max(P) \quad (10)$$

$$P = \frac{TP}{TP + FP} \quad (11)$$

Here,  $TP$  indicates the true positive and  $FP$  means the false positive value.

#### 4. Result Analysis and Discussion

The performance analysis of the OADLS-ALDC system is verified utilizing the leukemia classification dataset from Kaggle [25]. It includes 3875 images with 1927 normal and 1948 ALL samples as revealed in Table 1. Fig. 3 denotes the sample imageries. Fig. 4 indicates the segmented images and extracted features.

**Table 1** Details on database

Classes	No. of Samples
NORMAL	1927
Acute Lymphoblastic Leukemia (ALL)	1948
<b>Total Samples</b>	<b>3875</b>



# Power System Technology

ISSN:1000-3673

Received: 16-04-2023

Revised: 12-05-2023

Accepted: 07-06-2023

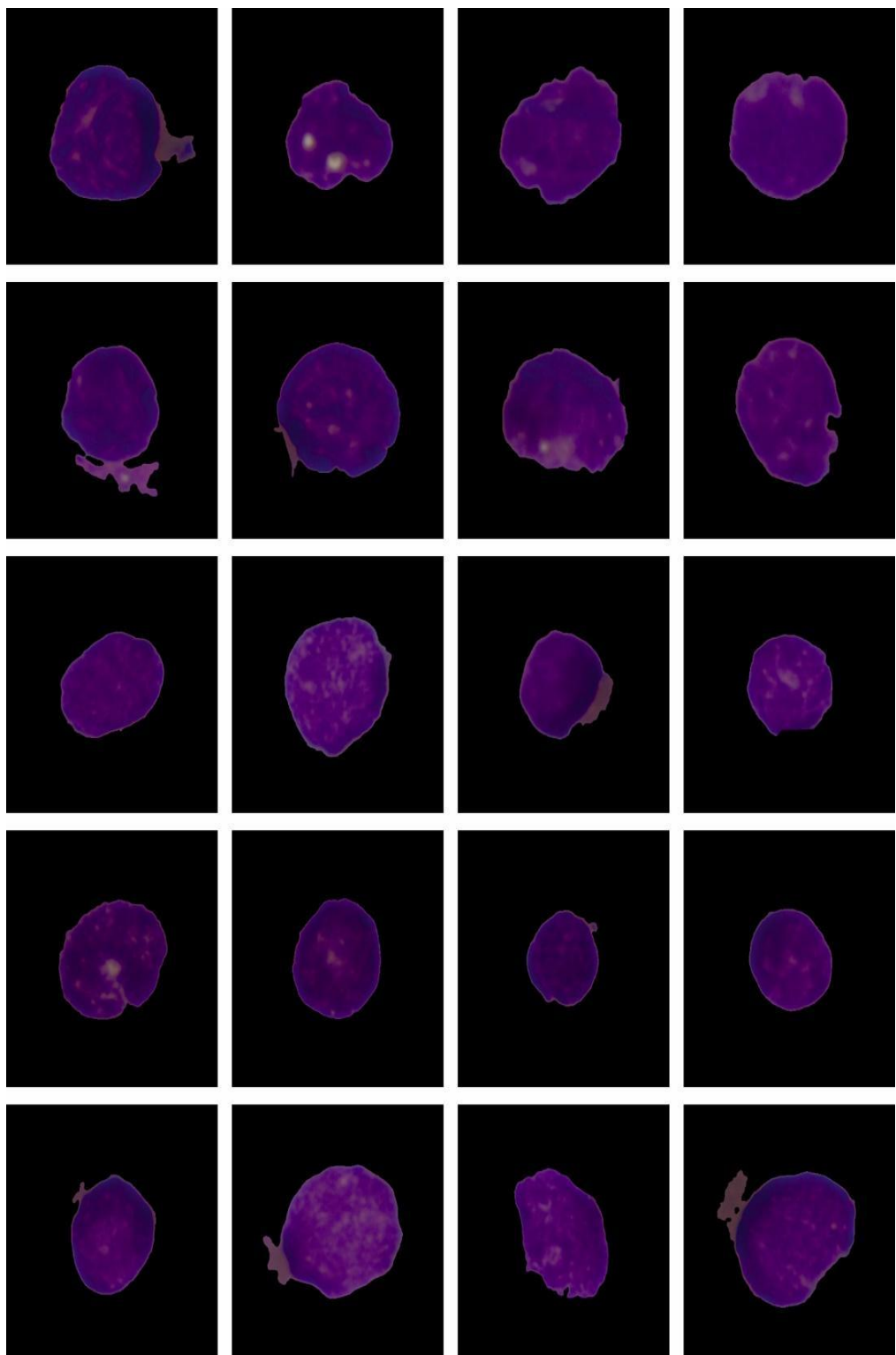


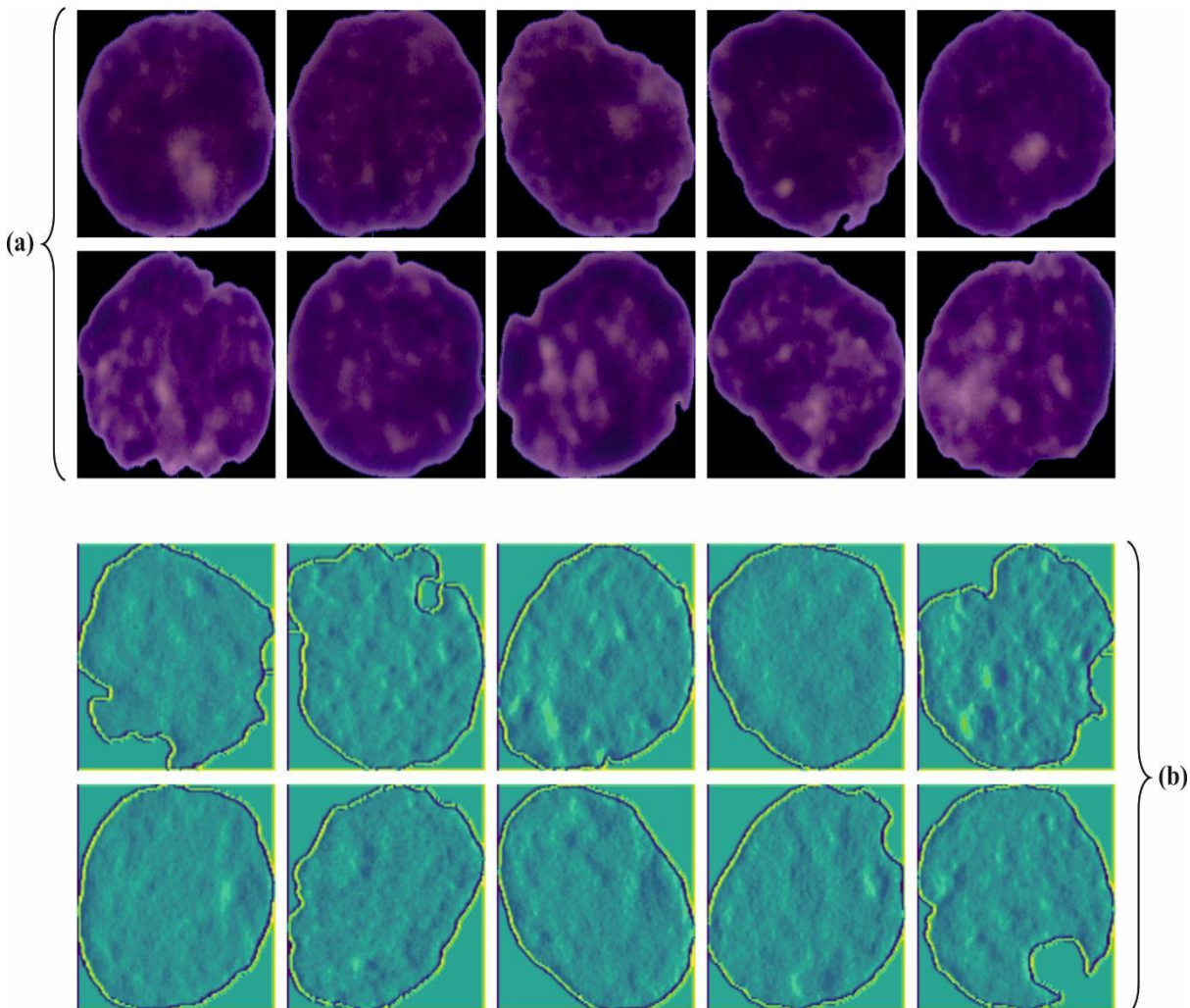
**Fig. 3.** Sample Images



Received: 16-04-2023

Revised: 12-05-2023

Accepted: 07-06-2023



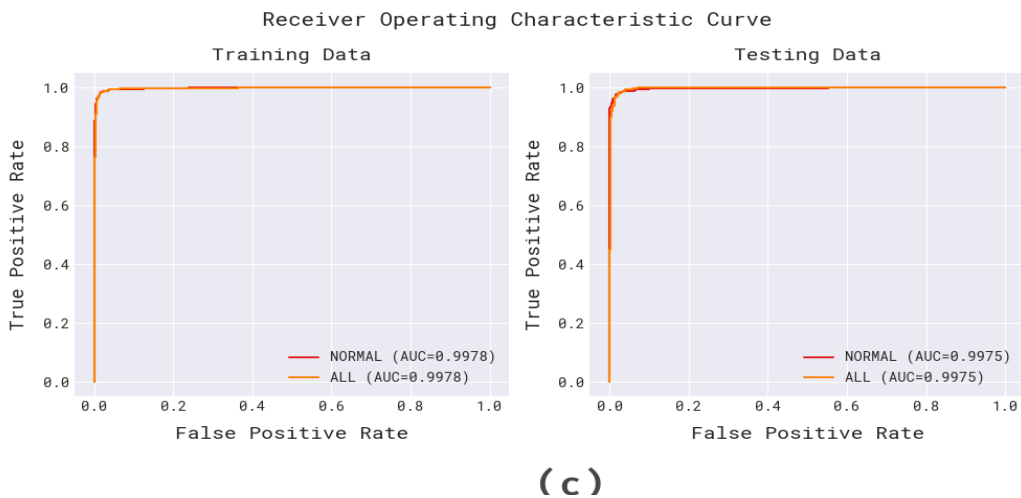
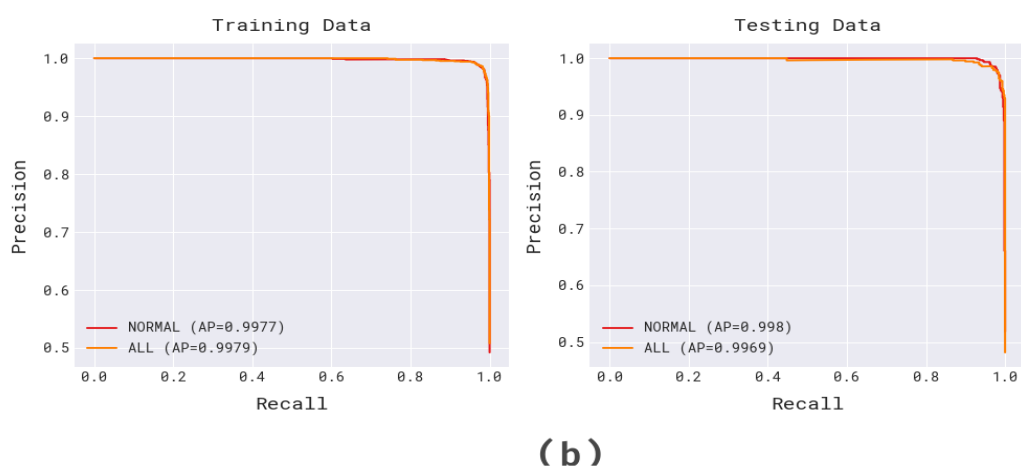
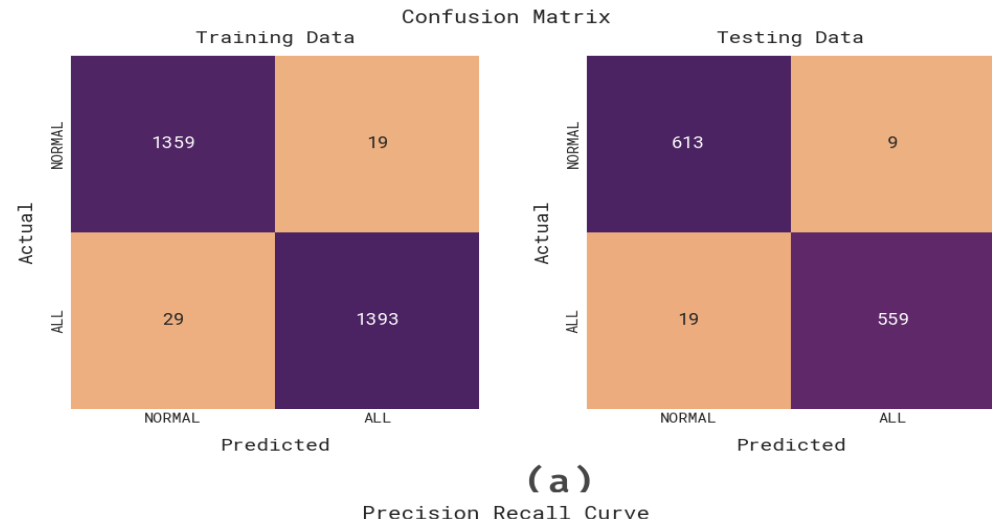
**Fig. 4.** a) Segmented Images b) Extracted Features

Fig. 5 shows the classifier results of the OADLS-ALDC approach under the training and testing data. Fig. 5a shows the confusion matrices presented by the OADLS-ALDC technique. The figure suggested that the OADLS-ALDC methodology has known and classified all 2 class labels exactly. Correspondingly, Fig. 5b describes the PR study of the OADLS-ALDC approach. The outcome is that the OADLS-ALDC system has expanded the maximum performance of PR under all class labels. Lastly, Fig. 5c exposes the ROC study of the OADLS-ALDC approach. The result shows that the OADLS-ALDC approach has risen in skilled results with the highest ROC values under various classes.

Received: 16-04-2023

Revised: 12-05-2023

Accepted: 07-06-2023



**Fig. 5.** Training and Testing Data a) Confusion Matrix b) Precision-Recall Curve c) ROC Curve

Received: 16-04-2023

Revised: 12-05-2023

Accepted: 07-06-2023

The overall leukemia detection results of the OADLS-ALDC technique are exhibited in Table 2. In Fig. 6, the results offered by the OADLS-ALDC technique during the training process are exhibited. The results emphasized that the OADLS-ALDC model correctly recognized the normal and ALL samples. With normal class, the OADLS-ALDC technique offers an  $acc_y$  of 98.29%,  $prec_n$  of 97.91%,  $sens_y$  of 98.62%,  $spec_y$  of 97.96%, and  $F1_{score}$  of 98.26%.

**Table 2** Leukaemia detection of OADLS-ALDC technique under training and testing data

Data Split	Measures	NORMAL	ALL	Overall
Training	<b>Accuracy</b>	98.29	98.29	98.29
	<b>Precision</b>	97.91	98.65	98.28
	<b>Sensitivity</b>	98.62	97.96	98.29
	<b>Specificity</b>	97.96	98.62	98.29
	<b>F1-Score</b>	98.26	98.31	98.29
Testing	<b>Accuracy</b>	97.67	97.67	97.67
	<b>Precision</b>	96.99	98.42	97.7
	<b>Sensitivity</b>	98.55	96.71	97.63
	<b>Specificity</b>	96.71	98.55	97.63
	<b>F1-Score</b>	97.77	97.56	97.66

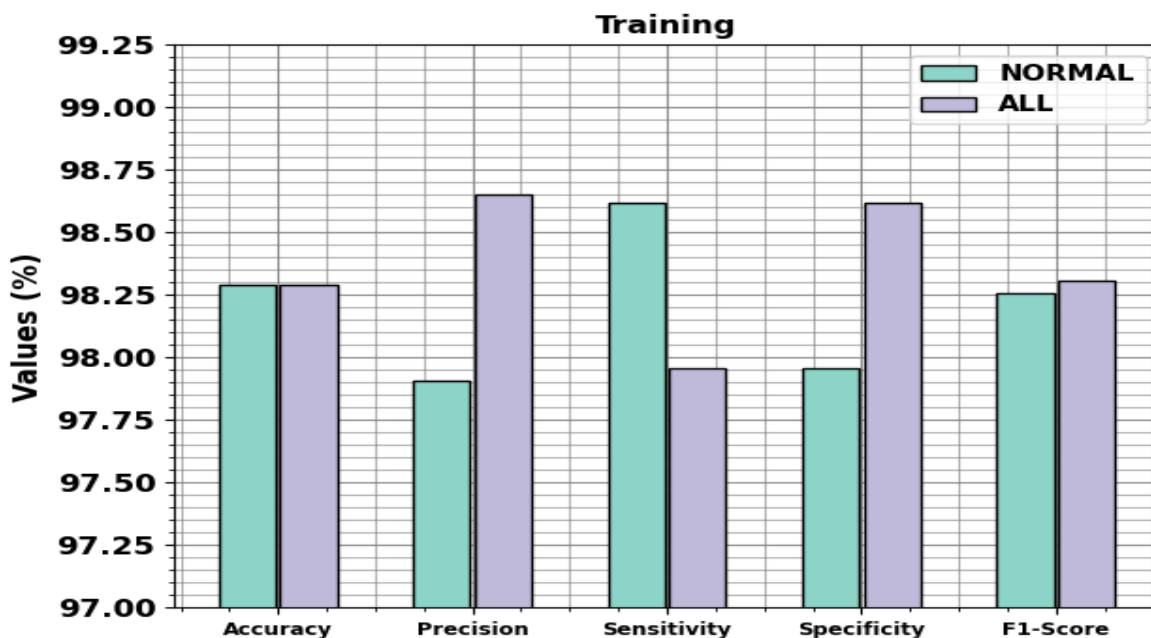


**Fig. 6.** Leukaemia detection of OADLS-ALDC technique under training data

In Fig. 7, the outcomes offered by the OADLS-ALDC system during the testing process are exhibited. The outcomes highlighted that the OADLS-ALDC approach properly recognized



Received: 16-04-2023

Revised: 12-05-2023

Accepted: 07-06-2023

the normal and ALL samples. With normal class, the OADLS-ALDC method delivers an  $accu_y$  of 97.67%,  $prec_n$  of 96.99%,  $sens_y$  of 98.55%,  $spec_y$  of 96.71%, and  $F1_{score}$  of 97.77%.

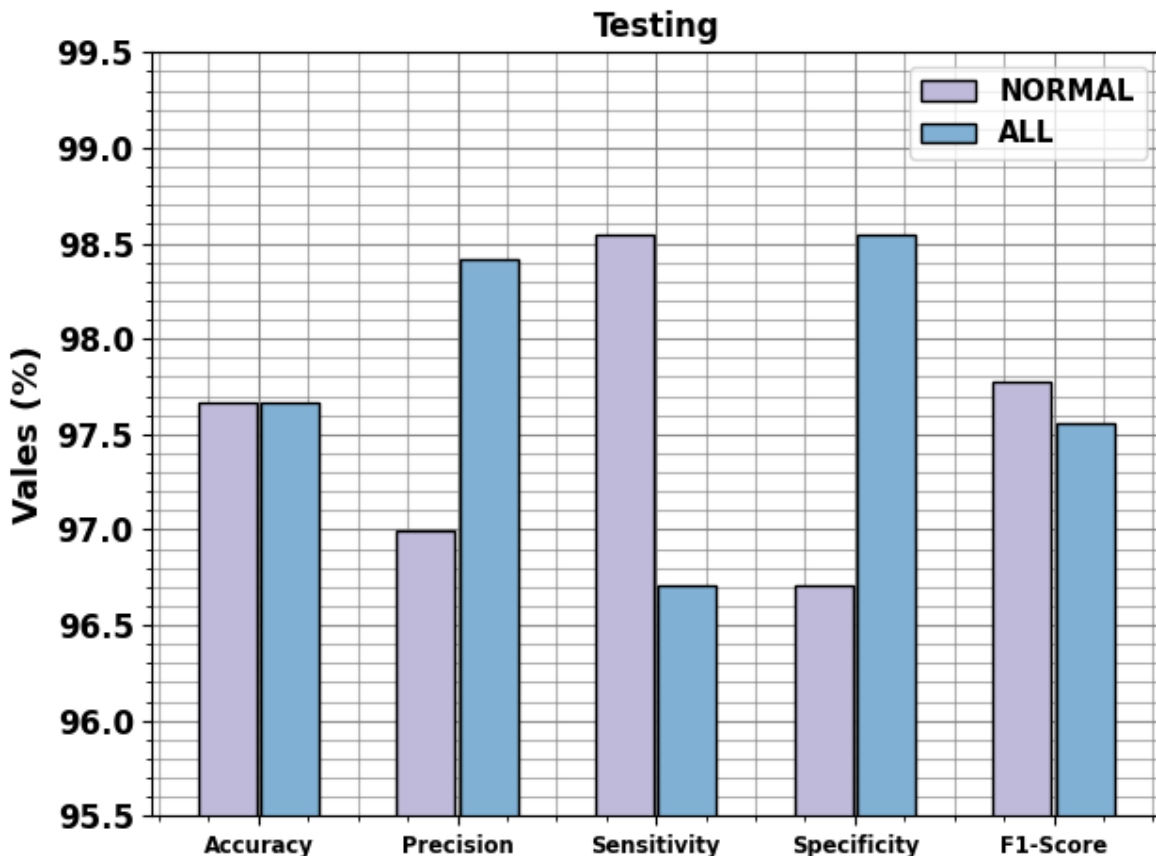


**Fig. 7.** Leukaemia detection of OADLS-ALDC technique under training data

The performance of the OADLS-ALDC system is presented in Fig. 8 in the type of validation accuracy (VALAC) and training accuracy (TRAAC) curves. The result shows a useful explanation of the behavior of the OADLS-ALDC approach over numerous epoch counts, signifying its learning technique and general proficiencies. Mainly, the outcome defines a constant growth in the VALAC and TRAAC with an evolution in epochs. It states the adaptive nature of the OADLS-ALDC methodology in the outline recognition system on both the data. The expanding tendency in VALAC condenses the capability of the OADLS-ALDC approach to adjust to the training data and is also best in distributing accurate identification of unseen data, representing strong generalization abilities.



Received: 16-04-2023

Revised: 12-05-2023

Accepted: 07-06-2023

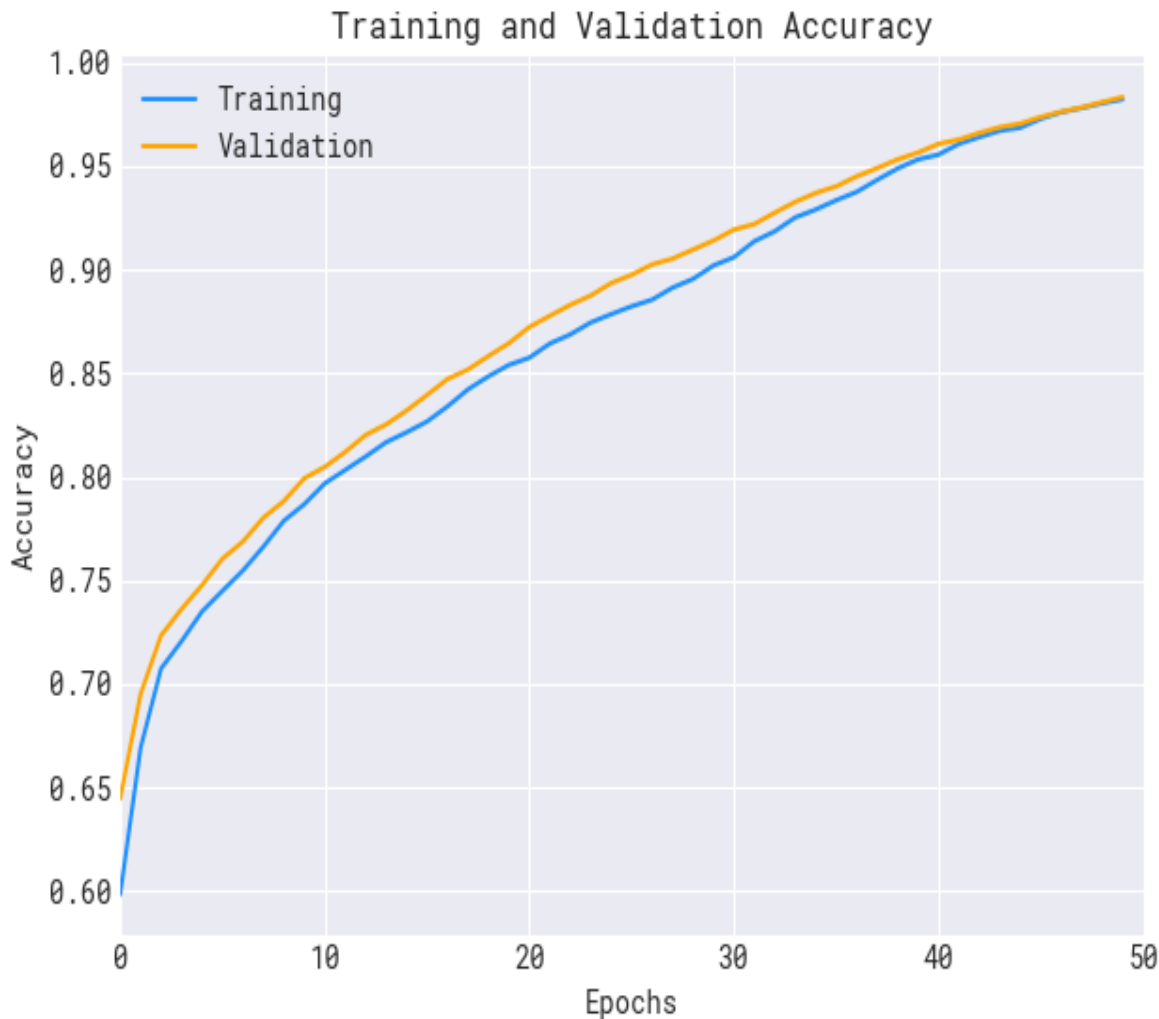


**Fig. 8.**  $Accu_y$  curve of the OADLS-ALDC technique

Fig. 9 exhibits an inclusive representation of the validation loss (VALLS) and training loss (TRALS) outcomes of the OADLS-ALDC system over separate epochs. The advanced reduction in TRALS emphasises the OADLS-ALDC method improving the weights and diminishing the classification error on the TRA and TES data. The outcome states a clear understanding of the OADLS-ALDC model's link with the TRA data, emphasizing its skill to take patterns within both datasets. Remarkably, the OADLS-ALDC technique regularly expands its parameters in decreasing the differences between the prediction and real TRA class labels.

Received: 16-04-2023

Revised: 12-05-2023

Accepted: 07-06-2023



**Fig. 9.** Loss curve of the OADLS-ALDC technique

The performance comparison of the OADLS-ALDC technique is reported in Table 3 [5, 26, 27]. In Fig.10, the outcomes of the OADLS-ALDC approach are compared with other techniques in terms of  $accu_y$ ,  $prec_n$ , and  $F1_{score}$ . The outcomes suggest that the CNN, VT, VGG16, DenseNet121, MobileNetV2, and InceptionV3 techniques have described the smallest performance. While, the CNN-ECA, GAO, and SVM-cell energy feature methods have accomplished moderately closer outcomes. Yet, the OADLS-ALDC system shows superior performance with the greatest  $accu_y$ ,  $prec_n$ , and  $F1_{score}$  of 98.29%, 98.28%, and 98.29%, correspondingly.

**Table 3** Comparative analysis of the OADLS-ALDC method with recent models

Models	$Accu_y$	$Prec_n$	$Sens_y$	$Spec_y$	$F1_{score}$
CNN Model	88.25	88.72	92.43	89.18	91.77
Vision Transformer	88.20	91.70	92.44	93.24	87.76
CNN-ECA Module	91.10	90.85	91.74	89.56	92.49



Received: 16-04-2023

Revised: 12-05-2023

Accepted: 07-06-2023

GAO-Based Method	93.84	89.01	91.82	91.67	88.22
SVM-Cell Energy Feature	94.00	92.20	91.32	88.99	93.88
VGG16 Model	87.30	86.40	96.70	89.57	91.30
DenseNet121	89.00	90.50	93.70	90.70	92.10
MobileNetV2	87.80	88.30	94.60	91.60	91.30
InceptionV3	84.00	87.10	89.80	91.27	88.40
OADLS-ALDC	98.29	98.28	98.29	98.29	98.29

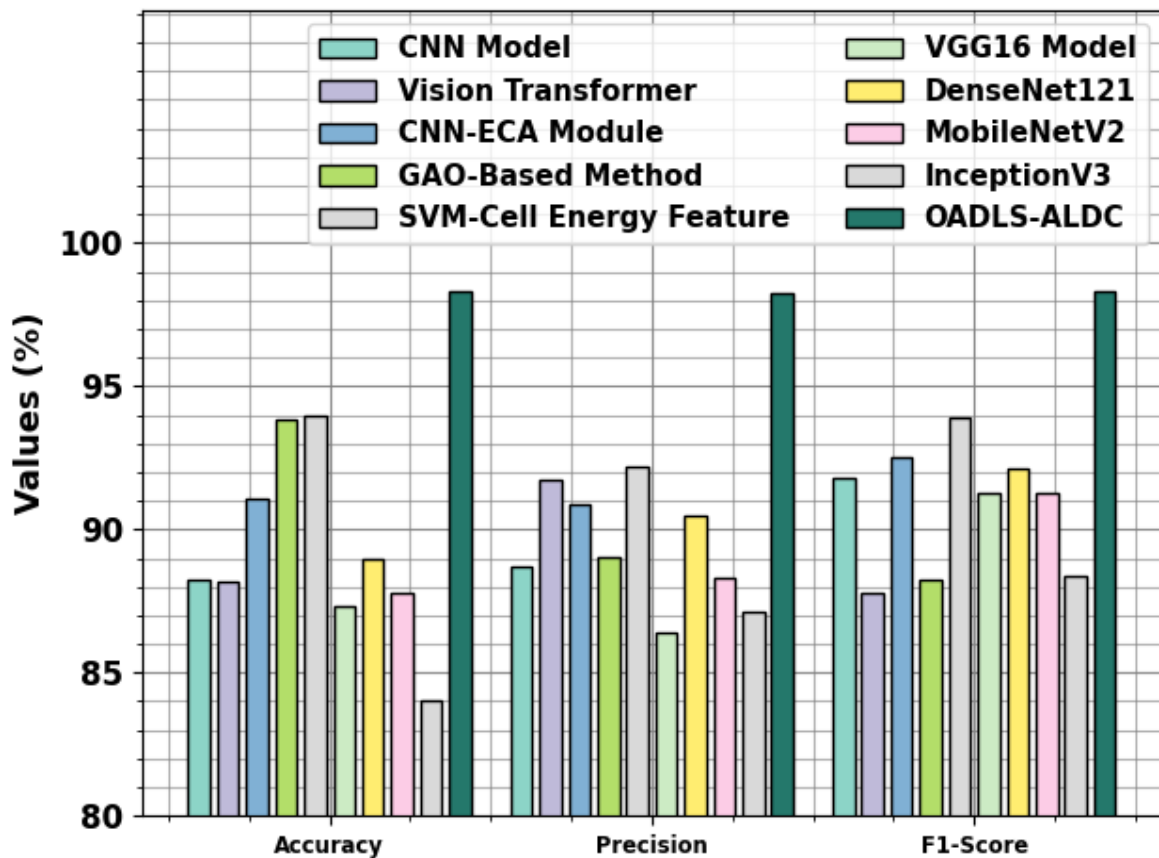


**Fig. 10.**  $Accu_y$ ,  $prec_n$ , and  $F1_{Score}$  analysis of OADLS-ALDC technique with recent models

In Fig. 11, the results of the OADLS-ALDC model are paralleled with other systems in terms of  $sens_y$ , and  $spec_y$ . The outcomes indicate that the CNN, VT, VGG16, DenseNet121, MobileNetV2, and InceptionV3 approaches have testified to minimum performance. Also, the CNN-ECA, GAO, and SVM-cell energy feature methods have accomplished moderately closer



Received: 16-04-2023

Revised: 12-05-2023

Accepted: 07-06-2023

outcomes. On the other hand, the OADLS-ALDC approach shows greater performance with the highest  $sens_y$ , and  $spec_y$  of 98.29%, and 98.29%, respectively.

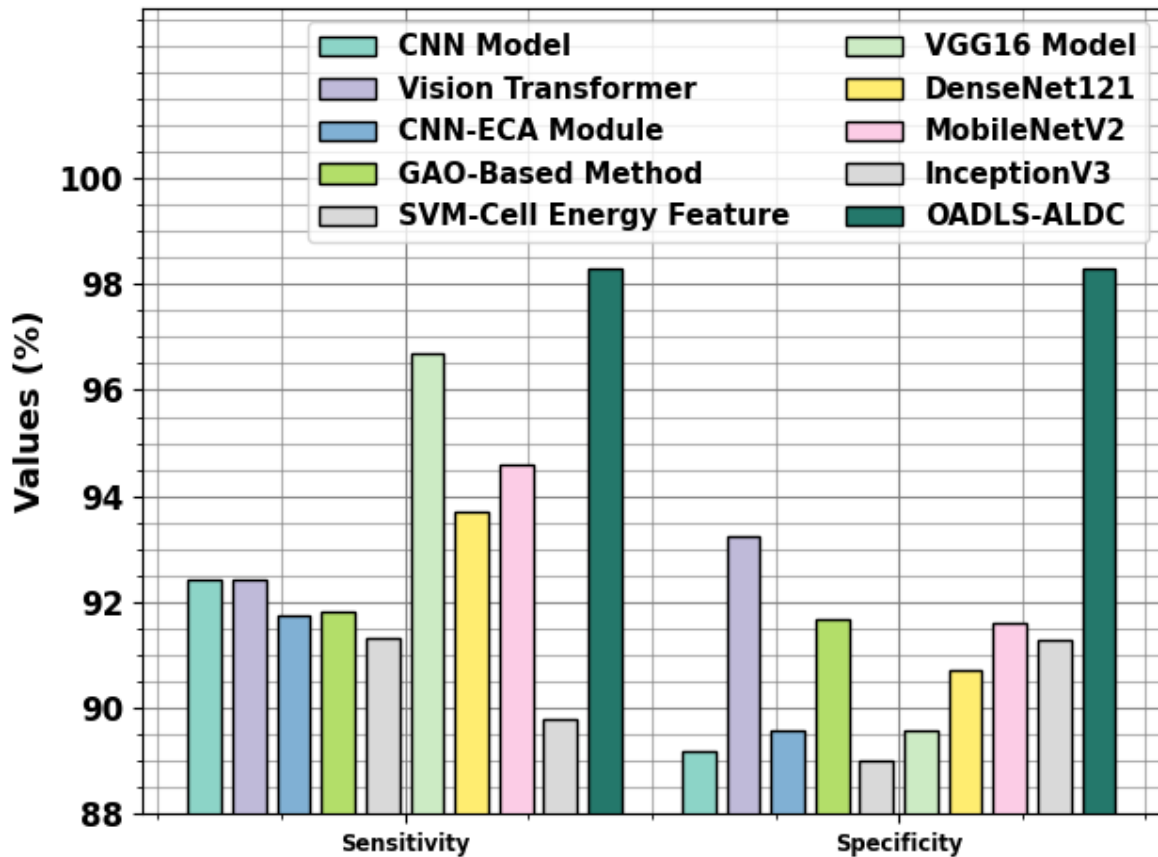


**Fig. 11.**  $Sens_y$  and  $spec_y$  analysis of OADLS-ALDC technique with recent models

## 5. Conclusion

In this study, we proposed an OADLS-ALDC technique. The main purpose of the OADLS-ALDC technique approach contains different kinds of processes involved as image processing, segmentation, feature extraction, ACRNN-based detection, and parameter selection. Primarily, the OADLS-ALDC technique undergoes image pre-processing in two phases: WF and DHE. At the same time, the Watershed Segmentation approach is applied to segment the pre-processed images. Next, the OADLS-ALDC technique uses EfficientNetV2M for the identification of useful feature vectors. Moreover, the recognition and identification of leukemia take place through the use of the ACRNN model. Furthermore, the hyperparameter selection of the ACRNN model is performed using RMSProp Optimizer. To highlight the improved detection outcomes of the OADLS-ALDC model, a sequence of experiments were



Received: 16-04-2023

Revised: 12-05-2023

Accepted: 07-06-2023

involved. The experimental values are definite that the OADLS-ALDC approach gets better performance over other techniques.

## References

- [1] Mallick, P.K., Mohapatra, S.K., Chae, G.S. and Mohanty, M.N., 2023. Convergent learning-based model for leukemia classification from gene expression. *Personal and Ubiquitous Computing*, 27(3), pp.1103-1110.
- [2] Abhishek, A., Jha, R.K., Sinha, R. and Jha, K., 2022. Automated classification of acute leukemia on a heterogeneous dataset using machine learning and deep learning techniques. *Biomedical Signal Processing and Control*, 72, p.103341.
- [3] Gondal, C.H.A., Irfan, M., Shafique, S., Bashir, M.S., Ahmed, M., Alshehri, O.M., Almasoudi, H.H., Alqhtani, S.M., Jalal, M.M., Altayar, M.A. and Alsharif, K.F., 2023. Automated Leukemia Screening and Sub-types Classification Using Deep Learning. *Computer Systems Science & Engineering*, 46(3).
- [4] Das, P.K. and Meher, S., 2021. An efficient deep convolutional neural network based detection and classification of acute lymphoblastic leukemia. *Expert Systems with Applications*, 183, p.115311.
- [5] Bukhari, M., Yasmin, S., Sammad, S., El-Latif, A. and Ahmed, A., 2022. A deep learning framework for leukemia cancer detection in microscopic blood samples using squeeze and excitation learning. *Mathematical Problems in Engineering*, 2022.
- [6] Hagar, M., Elsheref, F.K. and Kamal, S.R., 2023. A New Model for Blood Cancer Classification Based on Deep Learning Techniques. *International Journal of Advanced Computer Science and Applications*, 14(6).
- [7] Arivuselvam, B. and Sudha, S., 2022. Leukemia classification using the deep learning method of CNN. *Journal of X-ray science and technology*, 30(3), pp.567-585.
- [8] Ramagiri, A., Jahnvi, V., Gottipati, S., Monica, C., Afrin, S., Jyothi, B. and Chinnaiyan, R., 2023, March. Image Classification for Optimized Prediction of Leukemia Cancer Cells using Machine Learning and Deep Learning Techniques. In *2023 International Conference on Innovative Data Communication Technologies and Application (ICIDCA)* (pp. 193-197). IEEE.
- [9] Arivuselvam, B. and Sudha, S., 2022. Leukemia classification using the deep learning method of CNN. *Journal of X-ray science and technology*, 30(3), pp.567-585.
- [10] Abhishek, A., Jha, R.K., Sinha, R. and Jha, K., 2023. Automated detection and classification of leukemia on a subject-independent test dataset using deep transfer learning supported by Grad-CAM visualization. *Biomedical Signal Processing and Control*, 83, p.104722.
- [11] Ghongade, O.S., Reddy, S.K.S., Gavini, Y.C., Tokala, S. and Enduri, M.K., 2023. Acute Lymphoblastic Leukemia Blood Cells Prediction Using Deep Learning & Transfer



Received: 16-04-2023

Revised: 12-05-2023

Accepted: 07-06-2023

Learning Technique. *Indonesian Journal of Electrical Engineering and Informatics (IJEEI)*, 11(3), pp.778-790.

- [12] MoradiAmin, M., Yousefpour, M., Samadzadehaghdam, N., Ghahari, L., Ghorbani, M. and Mafi, M., 2024. Automatic classification of acute lymphoblastic leukemia cells and lymphocyte subtypes based on a novel convolutional neural network. *Microscopy Research and Technique*.
- [13] Rodrigues, L.F., Backes, A.R., Travençolo, B.A.N. and de Oliveira, G.M.B., 2022. Optimizing a deep residual neural network with genetic algorithm for acute lymphoblastic leukemia classification. *Journal of Digital Imaging*, 35(3), pp.623-637.
- [14] Ahmed, I.A., Senan, E.M., Shatnawi, H.S.A., Alkhraisha, Z.M. and Al-Azzam, M.M.A., 2023. Hybrid techniques for the diagnosis of acute lymphoblastic leukemia based on fusion of CNN features. *Diagnostics*, 13(6), p.1026.
- [15] Awais, M., Ahmad, R., Kausar, N., Alzahrani, A.I., Alalwan, N. and Masood, A., 2024. ALL classification using neural ensemble and memetic deep feature optimization. *Frontiers in Artificial Intelligence*, 7, p.1351942.
- [16] Abunadi, I. and Senan, E.M., 2022. Multi-method diagnosis of blood microscopic sample for early detection of acute lymphoblastic leukemia based on deep learning and hybrid techniques. *Sensors*, 22(4), p.1629.
- [17] Khan, S., Sajjad, M., Abbas, N., Escoria-Gutierrez, J., Gamarra, M. and Muhammad, K., 2024. Efficient leukocytes detection and classification in microscopic blood images using convolutional neural network coupled with a dual attention network. *Computers in Biology and Medicine*, p.108146.
- [18] Lew, K.L., Kew, C.Y., Sim, K.S. and Tan, S.C., 2024. Adaptive Gaussian Wiener Filter for CT-Scan Images with Gaussian Noise Variance. *Journal of Informatics and Web Engineering*, 3(1), pp.169-181.
- [19] Rao, B.S., 2020. Dynamic histogram equalization for contrast enhancement for digital images. *Applied Soft Computing*, 89, p.106114.
- [20] Li, J., Luo, W., Wang, Z. and Fan, S., 2019. Early detection of decay on apples using hyperspectral reflectance imaging combining both principal component analysis and improved watershed segmentation method. *Postharvest Biology and Technology*, 149, pp.235-246.
- [21] Shabrina, N.H., Lika, R.A. and Indarti, S., 2023. Deep learning models for automatic identification of plant-parasitic nematode. *Artificial Intelligence in Agriculture*, 7, pp.1-12.
- [22] Zhang, Z., Xu, S., Zhang, S., Qiao, T. and Cao, S., 2021. Attention based convolutional recurrent neural network for environmental sound classification. *Neurocomputing*, 453, pp.896-903.



Received: 16-04-2023

Revised: 12-05-2023

Accepted: 07-06-2023

- [23] Lee, S.H., Goëau, H., Bonnet, P. and Joly, A., 2020. Attention-based recurrent neural network for plant disease classification. *Frontiers in Plant Science*, 11, p.601250
- [24] Ahda, F.A.I., Wibawa, A.P., Prasetya, D.D. and Sulistyo, D.A., 2024. Comparison of Adam Optimization and RMS prop in Minangkabau-Indonesian Bidirectional Translation with Neural Machine Translation. *JOIV: International Journal on Informatics Visualization*, 8(1), pp.231-238.
- [25] <https://www.kaggle.com/datasets/andrewmvd/leukemia-classification>
- [26] Batool, A. and Byun, Y.C., 2023. Lightweight EfficientNetB3 model based on depthwise separable convolutions for enhancing classification of leukemia white blood cell images. *IEEE Access*.
- [27] Sulaiman, A., Kaur, S., Gupta, S., Alshahrani, H., Reshan, M.S.A., Alyami, S. and Shaikh, A., 2023. ResRandSVM: Hybrid Approach for Acute Lymphocytic Leukemia Classification in Blood Smear Images. *Diagnostics*, 13(12), p.2121.